LABORATORY Spotlight
Reprinted from NHMFL Reports Summer 2002
The National High Magnetic Field Laboratory
1800 East Paul Dirac Drive • Tallahassee, Florida 32310 • 850-644-0311 • http://www.magnet.fsu.edu

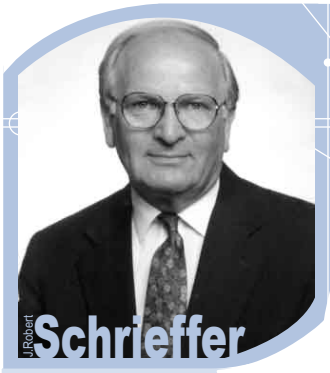

from the Chief Scientist's Desk

J.Robert Schrieffer

In this issue, Tom Mareci and coworkers discuss the remarkably detailed information that can be achieved concerning multiple rates of water self-diffusion and diffusion anisotropy in biological tissue. Using very high magnetic field, 14.1 and 17.6 T, they find in spinal cord tissue that there are important differences in the fast and slow diffusion tensors. The white matter margins around the gray matter exhibit the slowest average diffusivity in the white matter. They suggest that this is due to a higher packing density of microtubules in these axons compared to other axons in the white matter. In brain slices, the bi-exponential analysis of water diffusion giving the diffusion rates and volume fractions involved. To simulate the effect of ischemia, the slices were perfused with a Na+/K+ ATPase inhibitor that caused cell swelling. The diffusion rates did not change but the volume fractions did. These measurements clearly show how detailed information can be obtained in the spatially resolved diffusion of water in important biological material.

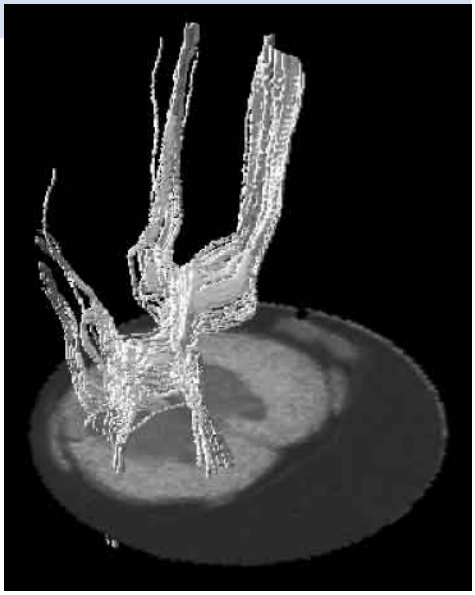

Experimental Observations of Multiple Rates of Water Self-Diffusion and Diffusion Anisotropy in Tissue, Intact Isolated Cells, and Cell Phantoms

T.H. Mareci, UF, Biochemistry and Molecular Biology, McKnight Brain Institute/NHMFL
S.C. Grant, UF, Neuroscience, McKnight Brain Institute/NHMFL
E. Ozarslan, UF, Physics, McKnight Brain Institute/NHMFL
P.E. Thelwall, UF, Neuroscience, McKnight Brain Institute/NHMFL
S.J. Blackband, UF, Neuroscience, McKnight Brain Institute/NHMFL

Introduction: Water in biological tissue diffuses within cells, in extracellular spaces, and crosses membranes. NMR imaging can be used to measure the translational diffusion of water using pulse-field-gradient spin echo methods. Using these results, the rate and direction of diffusion can be quantified. If the water is diffusing in a structured environment, like nerve fibers, this can be used to visualize the tissue structure. For example, we have used NMR measures of water translational diffusion to create a map of the nerve fibers (colored gray-blue) within a spinal cord (representative slice in orange) shown in Fig. 1.

This view of water translational diffusion in tissue, however, is simplistic. NMR imaging and spectroscopic studies at high diffusion-weighting ($b > 1500$ s/mm^2) have shown that cells and tissues exhibit exponential signal loss described by two or more rates of decay. These rates may reflect diffusion in extracellular and intracellular water compartments,[25, 19, 21, 10, 20, 23, 2, 18, 4] but the volume fractions do not appear to agree with those determined by other methods so the interpretation of these results is unclear. In order to better understand the

Figure 1. A map of the nerve fibers (colored gray-blue) within a spinal cord (representative slice in orange) created by NMR measures of water translational diffusion. (see *www.magnet.fsu.edu* for color presentation.)

physical meaning of the measured diffusion, we have been investigating multiple-component diffusion within intact whole tissue,[14] tissue slices,[6, 4] single isolated cells,[12, 7, 8, 22] and cell phantoms.[24] In the following, we will discuss our findings concerning the origins of the fast and slow components of a two-component fit to diffusion measurements.

Methods: We used the Kärger[15] model of two-component diffusion in the slow compartment-exchange limit for the analysis of our measurements. In the limit where the diffusion time, τ, is short compared to the life-time, $\tau_{1(2)}$, of water in either compartment 1 (extracellular?) or compartment 2 (intracellular?), i.e., $\tau << \tau_{1(2)}$, a two-rate decay will be observed with the following functional form,

$$S(b)/S_0 = f_1 \exp(-b D_1) + f_2 \exp(-b D_2) \quad , \quad [1]$$

where b represents the pulse-field-gradient diffusion weighting applied by the NMR measurement method.

Conversely, in the long diffusion-time limit, i.e., $\tau >> \tau_{1(2)}$, water in compartment 1 and compartment 2 will have mixed and a single effective rate of diffusion, D_{eff}, will be observed, which is an average of the rates of the two compartments weighted by the volume fractions of each compartment. In the intermediate time limit, i.e., $\tau \approx \tau_{1(2)}$, the signal decay is bi-exponential in character but has a more complex dependence on rates and times.[15] This model is valid for spatial compartments, such as intracellular and extracellular spaces, but the model also fits for compartments representing the local environment of the water.

Also, we extended the diffusion tensor imaging (DTI) formalism of Basser *et al.*[17] to account specifically for bi-exponential diffusion.[14] For mono-exponential diffusion, a series of diffusion-weighted images may be used to compute a single-rate DTI by fitting to:

$$\ln(S/S_0) = -\Sigma_{ij} b_{ij} D_{ij} \quad , \quad [2]$$

where b is the diffusion weighting factor, S is the diffusion-dependent signal intensity, S_0 is the (T_2-weighted) signal intensity in the absence of diffusion weighting gradients, b_{ij} is the i,jth element of the matrix of diffusion weighting terms,[17] D_{ij} is the i,jth element of the DTI, and i,j = x,y,z. For a two-compartment model under the assumption of slow exchange (i.e., minimal water exchanges between compartments during diffusion time), Eq. [2] may be expanded to a linear combination of observable signal components:[15]

$$S_{ij} = S_{0f} \exp(-\Sigma_{ij} b_{ij} D_{ijf}) + S_{0s} \exp(-\Sigma_{ij} b_{ij} D_{ijs}), \quad [3]$$

where S_{0f} and S_{0s} are the (T_2-weighted) signal intensities in the absence of diffusion weighting gradients and the subscripts f and s denote fast and slow components of diffusion, respectively.

Samples: Diffusion tensor images of the excised fixed rat spinal cords in phosphate buffered saline solution were measured at 14.1 T.[13, 14] For isolated single cells, the L7 neuron from the abdominal ganglion of *Aplysia californica* was extracted and maintained in artificial seawater.[22] NMR measurements were performed at very high magnetic fields (14.1 and 17.6 T) using small diameter solenoidal RF coils.[26] For perfused brain slices, NMR measurements at 14.1 T were obtained from 500-μm-thick coronal slices from the rat hippocampus using a standard 10 mm RF coil in a specially constructed slice holder.[3] For erythrocyte ghosts,[24] human blood was collected from a volunteer, and ghosts were prepared by gel filtration with hemolysis induced in a hypotonic solution. Diffusion-weighted MR spectra of the erythrocyte ghosts were measured at 17.6 T.

Results: Using multiple diffusion-weightings, we have quantified multiple-component diffusion rates in whole fixed tissue (intact fixed spinal cord), perfused tissue slices (rat hippocampus), perfused single cells (*Aplysia* neurons), and cell phantoms (blood cell ghosts). In addition, we have examined diffusion anisotropy in these whole fixed tissue samples and single cells. The measurements are summarized below.

Intact Spinal Cord (fixed): The fast and slow component diffusion tensors exhibit similar gross features, such as fractional anisotropy, in both white and gray matter.[14] There also are important differences, however, that appear to be consistent with differences in intracellular and extracellular structure. In particular, the slow diffusion-component tensor exhibits subtle features that seem to be closely related to the cellular and axonal cytoskeleton. For example, the white matter margins around the gray matter exhibit the slowest average diffusivity in the white matter. This is consistent with a higher packing density of microtubules in the axoplasm of these axons compared to other axons in white matter. But the volume fractions of the fast diffusion component (66 to 80%) and slow diffusion component (20 to 34%) were not consistent with commonly accepted values. These calculated volume fractions appear to be weighted by T_2 relaxation of water with the experimental parameters used in these measurements (i.e. echo time of 36 ms with a diffusion time of 17 ms).

Perfused Brain Slices (Rat Hippocampus): Bi-exponential analysis of water diffusion in hippocampal brain slices[4] yielded a fast component

($1.015 \pm 0.155 \times 10^{-3}$ mm^2 s^{-1}) and a slow component ($0.089 \pm 0.026 \times 10^{-3}$ mm^2 s^{-1}), with a calculated fast-rate volume fraction of 53.3 ± 6.4%. To simulate the effect of ischemia, the slices are perfused with 1 mM ouabain (a Na^+/K^+ ATPase inhibitor) that caused cell swelling. The measured rates of diffusion did not change, but the calculated volume fractions changed. The fast diffusion volume fraction decreased by 10% while the slow diffusion fraction increased by 10. A possible effect of exchange between compartments was investigated by varying the diffusion time. At diffusion times less than 12 ms, the diffusion rates are constant, but at 20 ms the rates appear to become slower, possibly due to exchange between compartments. The effect of T_2 relaxation was investigated by varying the echo time at a constant diffusion weighting time. The measured rate of diffusion appears to increase as the echo time is varied from 24 to 100 ms indicating a differential effect of relaxation in the different compartments.

In further experiments, the cell volume fraction in the hippocampal slices was estimated by adding a paramagnetic contract agent to the slice perfusate.[5] The estimated cell volume fraction was 66 ± 4%. To investigate the effect of cell shrinkage, 60-mM mannitol was added to the perfusate resulting in a 26% decrease in cell volume fraction. Further diffusion measurements[6] were performed on slices perfused with the excitatory amino acid, N-methyl-D-aspartate (NMDA). The two rates of diffusion observed did not change upon addition of NMDA, but the volume fraction of rapidly diffusing water increased by 5%. The effect of NMDA was blocked by pretreatment with its antagonist dizocilpine maleate (MK-801).

Isolated Single Cells (L7 neuron of Aplysia californica): The cytoplasm and nucleus are resolved (see Fig. 2, Part A) and have very different relaxation and diffusion properties.[22,1,11] No diffusion anisotropy was detected in either the cytoplasm or the nucleus.[11] A 20% hypotonic perturbation to these cells[12] resulted in a significant increase in T_2 relaxation time (~20 to 30%) for both the cytoplasm and nucleus. As shown in Fig. 2, Part B, approximately a single rate of water diffusion was observed in the nucleus but the diffusion in the cytoplasm was observed to occur at multiple rates.[8] Cytoplasmic diffusion has a fast component ($0.48 \pm 0.14 \times 10^{-3}$ mm^2 s^{-1}) and a slow component ($0.034 \pm 0.017 \times 10^{-3}$ mm^2 s^{-1}) with calculated volume fractions of 61.3 ± 11.2% and 31.7 ± 11.2%. In localized spectroscopy measurements, the osmolyte, betaine, is observed in only the cytoplasm[7] with single component diffusion.[9]

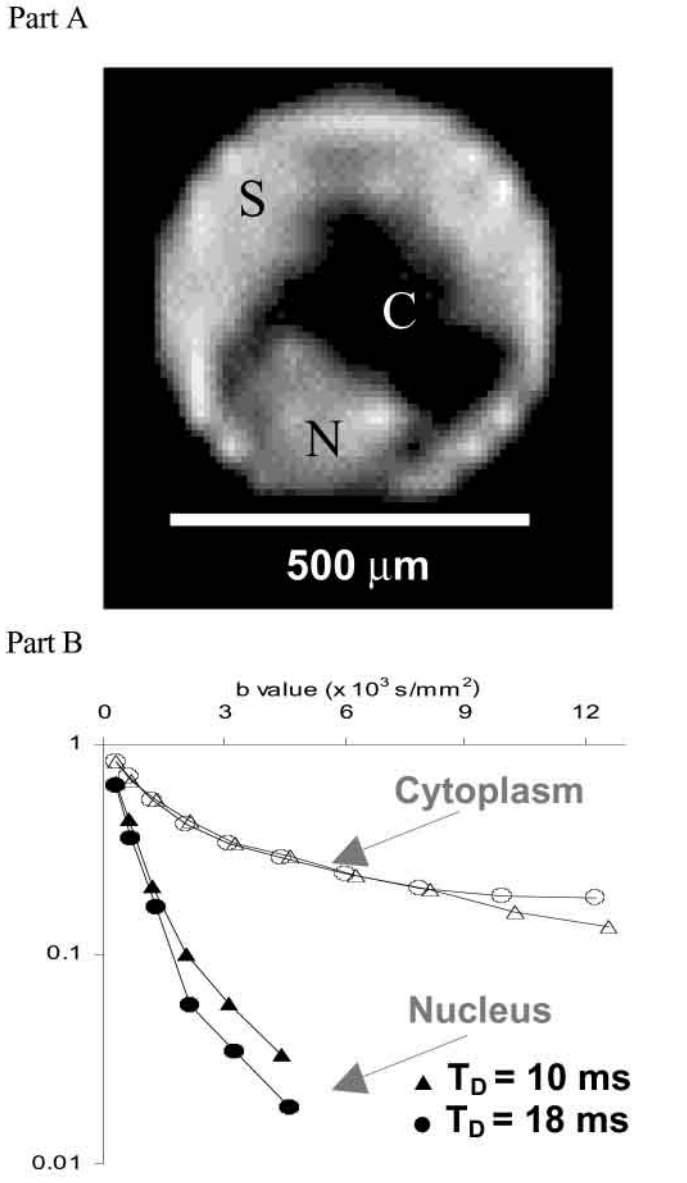

Figure 2A. Different relaxation and diffusion properties are resolved in the cell cytoplasm (C), cell nucleus (N), and artificial seawater (S) surrounding the cell.

Figure 2B. Water diffuses in the nucleus at a single rate, and at multiple

Erythrocyte Ghosts: Multi-component water diffusion was observed in ghost cell suspensions.[24] Data were fitted to a two-compartment model without including exchange as a first approximation to describe the data. The biophysical origins of the components separated by this analysis were investigated by observing the effects of cell density, membrane permeability, and cell size variation. The slow component appears to originate predominately from water molecules remaining in the intracellular compartment for the duration of the diffusion time, whereas the fast component is comprised

of water molecules in the extracellular compartment and undergoing transmembrane water exchange. This interpretation allows measurement of average cell dimensions; the apparent restriction demensions of water molecules in the slow component was 1.9 ± 0.2 μm. Additionally, the mean intracellular residence time of water (determined by membrane permeability) was calculated as 21.9 ± 1.3 ms for normal ghosts, and 45 ms after treatment with the aquaporin blocker, pCMBS.

Discussion and Conclusions: In all the tissues studied here, at least two diffusion components were observed (i.e., intermediate to slow exchange). The slow-exchange two-component model of water diffusion has been used to interpret the results of these tissue studies. The hypothesis that the fast component of water is solely extracellular and the slow component is solely intracellular appears to be naive. The two-compartment model in the slow exchange regime has two distinct limitations: (1) no slower diffusion rates are included, and (2) the model does not include exchange. To address the first limitation, slower rates of diffusion may be investigated but will require higher diffusion weighting (>10,000 s/mm^2) and greater signal-to-noise ratio than were available for most of these measurements. The inclusion of exchange in the model requires additional knowledge or the ability to measure exchange. Exchange can be measured in the erythrocyte ghosts so this system represents a simplified yet controllable model to explore the contribution of exchange and other factors. A possible alternative view, however, suggests that the bulk of the slowly diffusing water might be associated with macromolecules and membranes whereas water diffusing around the spaces established by these macromolecules and membranes constitutes the bulk of the rapidly diffusing water. If true, this view may help explain the observation of two-component diffusion in the cytoplasm.

The dependence of the MR measurement on relaxation poses an addition complication for the analysis of results. The choice of pulse sequence parameters (echo time) can lead to the distortion of compartment fractions due to relaxation and exchange effects. Also, the choice of the diffusion time can lead to exchange effects for the long diffusion time acquisitions.

The origin of diffusion anisotropy must be examined with care. Water diffusion in the *Aplysia* neurons was shown to be isotropic, but this may not be true for cells with extremely anisotropic membrane and/or cytoskeletal structure (e.g. axons). The fast and slow components of diffusion in the spinal cord were shown to be anisotropic with the slow component suggestive of intracellular processes. As stated above, however, a possible alternative view suggests another role for the bulk of the slowly diffusion water. Clearly, the results of compartmental modeling applied to tissue must be interpreted with great care and may be illuminated by the further development of tissue models.[23, 16]

[1] Aiken, N.R.; Hsu E.W.; Horsman, A. and Blackband, S.J., *Am. J. Physiol.*:*Cell Physiol.,* 271; **40**, C1295-C1302 (1996).
[2] Assaf,Y. and Cohen, Y., *J. Magn. Reson.,* **131**, 69-85 (1998).
[3] Blackband, S.J.; Bui, J.D.; Buckley, D.L.; Zelles, T.; Plant, H.D.; Inglis, B.A. and Phillips, M.I., *Magn. Reson. Med.*, **38**, 1012-1015 (1997).
[4] Buckley, D.L.; Bui, J.D.; Phillips, M.I.; Zelles, T.; Inglis, B.A.; Plant, H.D. and Blackband, S.J., *Magn. Reson. Med.*, **41**, 137-42 (1999).
[5] Buckley, D.L.; Bui, J.D.; Phillips, M.I. and Blackband, S.J., *Magn. Reson. Med.*, **42**, 603-607 (1999).
[6] Bui, J.D.; Buckley, D.L.; Phillips, M.I. and Blackband, S.J., *Neuroscience*, **93**, 487-490 (1999).
[7] Grant, S.C.; Aiken, N.R.; Plant, H.D.; Gibbs, S.; Mareci, T.H.; Webb, A.G. and Blackband S.J., *Magn. Reson. Med.,* **44**, 10-22 (2000).
[8] Grant, S.C.; Buckley, D.L.; Gibbs, S.; Webb, A.G. and Blackband, S.J., *Magn. Reson. Med.,* **46**, 1107-1112 (2001).
[9] Grant, S.C. and Blackband, S.J., in preparation for publication (2002)
[10] Helmer, K.F.; Dardzinski, B.J. and Sotak, C.H., *NMR Biomed*, **8**, 297-306 (1995).
[11] Hsu, E.W., Aiken, N.R. and Blackband, S.J., *Am. J. Physiol.,* 1996; 271 *Cell Physiol.*;40:C1895-C1900.
[12] Hsu, E.W.; Aiken, N.R. and Blackband, S.J., *Magn. Reson. Med.*, **37**, 624-427 (1997).
[13] Inglis, B.A.; Yang, L.; Wirth, III, E.D.; Plant, D., and Mareci, T.H., *Magn. Reson. Imag.,* **15**, 441-450 (1997).
[14] Inglis, B.A.; Bossart, E.L.; Buckley, D.L.; Wirth, III, E.D., and Mareci, T.H., *Magn. Reson. Med.,* **45**, 580-587 (2001).
[15] Kärger, J.; Pfeifer, H. and Heink, W., *Adv. Magn. Reson.*, **12**, 1-89 (1988).
[16] Li, J.G.; Stanisz, G.J. and Henkelman, R.M., *Magn. Reson. Med.*, **40**, 79-88 (1998).
[17] Mattiello, J.; Basser, P.J. and LeBihan, D., *J. Magn. Reson.*, **A108**,131-141 (1994).
[18] Mulkern, R.V.; Gudbjartsson, H.; Westin, C.-F.; Zengingonul, H.P.; Gartner, W.; Guttmann, C.R.; Robertson, R.L.; Kyriakos, W.; Schwartz, R.; Holtzmann, D.; Jolesz, F.A. and Maier, S.E., *NMR Biomed,* **12**, 51-62, (1999).
[19] Neeman, M.; Jarrett, K.A.; Sillerud, L.O. and Freyer, J.P., *Cancer Res*, **51**, 4072-9 (1991).
[20] Niendorf, T.; Dijkhuizen, R.M.; Norris, D.G.; van Lookeren-Campagne, M. and Nicolay, K., *Magn. Reson. Med.*, **36**, 847-857 (1996).
[21] Norris, D.G. and Niendorf T., *NMR Biomed*, **8**, 280-288 (1995).
[22] Schoeniger, J.S.; Aiken, N.; Hsu, E. and Blackband, S.J., *J. Magn. Reson. B,***103**, 261-273 (1994).
[23] Stanisz, G.J.; Szafer, A.; Wright, G.A. and Henkelman, R.M., *Magn. Reson. Med.,* **37**, 103-111 (1997).
[24] Thelwall, P.E.; Grant, S.C. and Blackband, S.J., in press, *Magn. Reson. Med.,* (2002).
[25] van Zijl, P.C.M.; Moonen, C.T.W.; Faustino, P.J.; Kaplan, O. and Cohen, J.S., *Proc. Natl. Acad. Sci. USA,* **88**, 3228-3232 (1991).
[26] Webb, A. and Grant S.J., *Magn. Reson.*, **113**, 83-87 (1996).